IEEE Access
Multidisciplinary | Rapid Review | Open Access Journal

Received February 21, 2019, accepted March 10, 2019, date of publication March 25, 2019, date of current version April 18, 2019.

Digital Object Identifier 10.1109/ACCESS.2019.2907179

A Hybrid Adaptive Control Strategy for Industrial Robotic Joints

BIN REN[1], YAO WANG[1], XURONG LUO[1], AND ROGELIO LOZANO[2]
[1]School of Mechatronic Engineering and Automation, Shanghai Key Laboratory of Intelligent and Robotics, Shanghai University, Shanghai 200444, China
[2]Centre National de la Recherche Scientifique, University de Technology of Compiègne, 60203 Compiègne, France

Corresponding author: Yao Wang (wangyao9504@126.com)

This work was supported in part by the National Natural Science Foundation of China under Grant 51775325, in part by the Young Eastern Scholars Program of Shanghai under Grant QD2016033, and in part by the Hong Kong Scholars Program of China under Grant XJ2013015.

ABSTRACT This paper presents a hybrid adaptive approximation-based control (HAAC) strategy for a class of uncertain robotic joints' system. The proposed control structure consists of a robust sliding mode controller and an adaptive approximation-based controller. The robust sliding mode controller is designed by using the super-twisting algorithm, which is a particularly effective method to decrease the chattering caused by the traditional sliding mode control (SMC) and compensate the disturbances. Another improvement of the robust sliding mode controller is that the robust control parameters only subject to the upper bound of the derivative of the external disturbances, rather than choosing a relatively large value. Moreover, the designed adaptive approximation-based controller has the following two distinctive features: 1) the control parameters are designed to be adjusted in real time and 2) the prior knowledge of actual robotic model is not required to be known. These features contribute to compensating the uncertainties. The stability of the closed-loop system is proved by using the Lyapunov theory, and the simulation results demonstrate the effectiveness of the proposed control method. Finally, the proposed HAAC could apply in the experiments of industrial robotic joints' system.

INDEX TERMS Hybrid adaptive control, robust sliding mode control, approximation-based control, robotic joints system.

I. INTRODUCTION

In recent years, the control design of trajectory tracking of robotic system have received considerable attention due to they are widely used in manufacturing, aerospace and other intelligent fields. The controller should be designed ensure the stability of robotic system. Moreover, the state variables (position and velocity) of joints must be able to track the desired trajectory by giving the driving torques [1]. For the past few years, many classic control methods, such as proportional derivative (PD) control, robust control and sliding mode control (SMC), have been used in the design of controller due to their unique merits. PD control is the most common method due to its simple structure and easy implementation [2]. Pan *et al.* [3] and Pan and Yu [4] presented a hybrid feedback feedforward (HFF) adaptive approximation-based control (AAC) method, which the PD controller was introduced to guarantee the stability of robotic system. Rubio *et al.* [5], [6] employed the PD controller to get that each manipulator link follows each desired reference. The proportional gain and derivative gain were independently subjected to each control input and output. Different from the PD control, robust control aims to achieve robust performance and stability in the presence of uncertainties. Guan *et al.* [7] utilized the robust controller to mitigate approximation-based errors of the dynamic models. Rubio [8] presented a robust feedback linearization method that makes it easier to find the control gains by only utilizing the main states feedbacks. Another widely used method, SMC, is insensitive to the parameter variation or external disturbances, and has a fast transient response [9], [10]. Based on these merits, Islam and Liu [11] presented a multi-parameter mode-based sliding mode method to improve the tracking performance for a certain class of nonlinear mechanical systems. Wang *et al.* [12] presented a continuous SMC method for a class of mismatched time-varying disturbances in compliantly actuated robots, and employed a generalized proportional integral observer to estimate the unknown disturbances. Pan *et al.* [13] proposed a singular perturbation-based continuous SMC strategy for a compliant robot arm driven

The associate editor coordinating the review of this manuscript and approving it for publication was Yongping Pan.

by the series elastic actuator, and used a second-order SMC technique to design the continuous SMC law. In addition, there are neural networks control [14], fuzzy control [15], iterative learning control [16], etc.

Nevertheless, industrial robotic joint is a Multiple-Input and Multiple-Output (MIMO) system with nonlinear, strong coupling and time varying [17], [18]. Uncertainties such as modeling errors, joint frictions and external disturbances degrade the control system's performance. Thus, more studies focus on developing new control strategies that combine multiple classic methods to compensate for the deficiencies of the single approach. Jiang and Zhang [19] presented a control method that uses an adaptive controller to estimate the control gains of the proportional-integral-derivative (PID) control, i.e., the fixed gains of classic PID was converted into the variable gains. This method improved the dynamic performance of PID control. However, this method relied on the accuracy of robotic model. It was difficult to obtain the accuracy model due to the presence of uncertainties. Zhang and Zhang [20] utilized a fuzzy controller to compensate the uncertainties of robotic system, and the approximation errors was eliminated by a robust controller. This method was dealt with a class of uncertainties of robotic system, but the chattering introduced by the robust term was still serious. Xi *et al.* [21] introduced a variable exponent trending law in the sliding mode controller, which successfully decreased the chattering. In this controller, the bounds of modeling errors were assumed to be a small constant, however, the actual robotic model was difficult to measure. Neila and Tarak [22] presented an adaptive robust controller to estimate the upper bound of uncertainties, and the tracking errors were eliminated by a continuous terminal sliding model controller. The prior knowledge of parameters uncertainty was not needed in this controller. The control torques still had a larger fluctuation in the initial stage, even if the chattering was decreased. Obviously, these methods still had some limitations, such as inaccurate model, severe chattering, inaccurate bounds of modeling errors, and large fluctuation.

To deal with these problems, a hybrid adaptive approximation-based control (HAAC) strategy is proposed in this paper. This hybrid adaptive controller is a new control structure, which includes a robust sliding mode controller and an adaptive approximation-based controller. The proposed control strategy has the following main contributions.

1) Considering an actual robotic joints system, the difficulty of the controller design is that the model parameters are time-varying. In this paper, an adaptive approximation-based controller is designed to estimate the actual robotic parameters, and thus the prior knowledge of robotic model is not required in this controller. Moreover, the control parameters are adjusted in real time to deal with the impact of uncertainties.
2) A robust controller is designed by using super-twisting algorithm. This control method has the following advantages. Firstly, it is robust to the external disturbances and system uncertainties. Secondly, it only requires the information of the sliding variable. Thirdly, the chattering caused by the traditional SMC can be effectively decreased. Moreover, the robust control parameters only subject to the upper bound of the derivative of the external disturbances, rather than choosing a relatively large value.
3) The stability of the closed-loop system in this paper can be ensured by using Lyapunov theory, and the effectiveness of the proposed control method is proved by a two-joint robotic system.

Moreover, a torsional vibration experiment on the robotic joints is proposed in this paper in order to test the influence of the input torques. Usually, there are four rotate vector (RV) reducers and two harmonic reducers in an industrial six-axis robot. These reducers directly affect the performance of trajectory tracking. However, most of studies on trajectory tracking such as in [23]–[27] are based on dynamic models and simulations, and a few studies have considered the vibration of the reducer inside the joints. Therefore, a torsional vibration test on the RV reducer, which is in the pedestal, is performed in this paper.

The paper is organized as follows: after the introduction, Section II describes the dynamics of robotic joints system and gives the control design and stability analysis. Section III presents the simulation results for a two-joint robotic system, verifying the effectiveness of the proposed controller. Section IV shows the torsional vibration experiment on the robotic joints. Finally, the conclusions and future works are given in Section V.

II. MODELING AND CONTROL SYSTEM

A. DYNAMICS OF ROBOTIC JOINTS SYSTEM

The industrial robotic manipulators adopt the structure of multiple connecting rod hinged in series, and the servo motors are installed inside the joints. Considering an n-joint industrial robotic system, its dynamic model can be described by the following second-order nonlinear differential equation [28], [29].

$$D(q)\ddot{q} + C(q, \dot{q})\dot{q} + G(q) + \tau_d(t) = \tau(t) \tag{1}$$

where $q(t), \dot{q}(t), \ddot{q}(t) \in \mathbb{R}^n$ are the vectors of joint angular positions, velocities and accelerations, respectively. $D(q) \in \mathbb{R}^{n\times n}$ is a symmetric positive definite inertia matrix, $C(q, \dot{q})\dot{q} \in \mathbb{R}^n$ is the centrifugal and Coriolis torques, $G(q) \in \mathbb{R}^n$ is the vector of gravitational torques, and $\tau(t) \in \mathbb{R}^n$ is the vector of control torques. $\tau_d(t) \in \mathbb{R}^n$ is the external disturbances bounded by $|\tau_d(t)| \leq \varepsilon_D$, where $\varepsilon_D \in \mathbb{R}^+$ is a constant indicating the upper bound of the external disturbances.

In general, the robotic system (1) has the following properties.

Property 1 [13], [14]: The matrix $D(q)$ is a symmetric positive-definite and satisfies $m_1\|x\|^2 \leq x^T D(q)\, x \leq m_2\|x\|^2$, $\forall x \in \mathbb{R}^n$, where $m_1, m_2 \in \mathbb{R}^+$ are the constants.

Property 2 [13], [28]: The matrix $\dot{D}(q) - 2C(q, \dot{q})$ is skew symmetric such that $x^T\left(\dot{D}(q) - 2C(q, \dot{q})\right)x = 0$, $\forall x \in \mathbb{R}^n$.

Property 3 [10]: The desired trajectory $q_d(t) \in \mathbb{R}^n$ is a twice continuously differentiable function in terms of t.

Property 4 [13]: $\dot{\tau}_d(t)$ exist and satisfies $|\dot{\tau}_d(t)| \leq \varepsilon_d$, where $\varepsilon_d \in \mathbb{R}^+$ is a constant indicating the upper bound of the derivative of the external disturbances.

The control objective is to design a controller for robotic system (1) under Properties 1-4 such that $q(t)$ will be able to track $q_d(t)$ while ensuring the stability of the closed-loop system.

B. CONTROL DESIGN

The position errors $e(t)$ and the derivative of position errors $\dot{e}(t)$ are defined as follows:

$$e(t) = q(t) - q_d(t) \tag{2}$$
$$\dot{e}(t) = \dot{q}(t) - \dot{q_d}(t) \tag{3}$$

The sliding mode function $s(t)$ is designed as follows:

$$s(t) = \dot{e}(t) + \Lambda e(t) \tag{4}$$

where Λ is a positive definite matrix indicating the sliding mode coefficient.

The control laws are designed as follows:

$$\tau = u_a + u_r + u_f \tag{5}$$
$$u_a = \hat{D}\ddot{q}_d + \hat{C}\dot{q}_d + \hat{G} - \hat{D}\Lambda\dot{e} - \hat{C}\Lambda e \tag{6}$$
$$u_r = -\kappa_1 |s|^{\frac{1}{2}} sgn(s) - \int \kappa_2 sgn(s)\, dt \tag{7}$$
$$u_f = -K_f s \tag{8}$$

where $u_a + u_f \in \mathbb{R}^n$ is the approximation-based controller, $u_r \in \mathbb{R}^n$ is the robust controller by using the super-twisting algorithm. $\hat{D}$, $\hat{C}$ and $\hat{G}$ are the estimated matrices of D, C and G, respectively. $\kappa_1 > 0, \kappa_2 > \varepsilon_d > 0$. K_f is a positive definite matrix.

In practice, the accurate dynamic models of robotic system are difficult to establish due to the presence of uncertainties. Therefore, the adaptive controller described in (9) is designed to estimate the model parameters.

$$\dot{\hat{P}} = -\Gamma^{-1}\Phi^T(q, \dot{q}, \dot{q}_r, \ddot{q}_r)\, s \tag{9}$$

where $\dot{q}_r = \dot{q}_d - \Lambda e$, $\ddot{q}_r = \ddot{q}_d - \Lambda\dot{e}$, and $\Phi(q, \dot{q}, \dot{q}_r, \ddot{q}_r) \in \mathbb{R}^{n\times m}$ is a regressor matrix for joint variables. $P \in \mathbb{R}^n$ represents the unknown model parameters. Γ is a positive definite matrix.

The following proof is given to show the Lyapunov stability of the robotic joints system (1) driven by the controller (5)-(9). Considering the positive definite function described in (10) as a Lyapunov function candidate.

$$V(t) = \frac{1}{2}s^T D s + \frac{1}{2}\tilde{P}^T\Gamma\tilde{P} \tag{10}$$

where $\tilde{P} = \hat{P} - P$, $\hat{P}$ is the estimate value of P, P is a constant vector, thus $\dot{\tilde{P}} = \dot{\hat{P}}$.

Differentiating of $V(t)$ with respect to time, we have

$$\begin{aligned}\dot{V}(t) &= s^T D\dot{s} + \frac{1}{2}s^T\dot{D}s + \tilde{P}^T\Gamma\dot{\tilde{P}} \\ &= s^T(D\ddot{q} - D\ddot{q}_d + D\Lambda\dot{e}) + \frac{1}{2}s^T\dot{D}s + \tilde{P}^T\Gamma\dot{\tilde{P}}\end{aligned} \tag{11}$$

where $\dot{s} = \ddot{e} + \Lambda\dot{e} = \ddot{q} - \ddot{q}_d + \Lambda\dot{e}$.

Substituting (1) into (11), we have

$$\begin{aligned}\dot{V}(t) = s^T[\tau - C(s + \dot{q}_d - \Lambda e) - G - \tau_d - D\ddot{q}_d \\ + D\Lambda\dot{e}] + \frac{1}{2}s^T\dot{D}s + \tilde{P}^T\Gamma\dot{\tilde{P}}\end{aligned} \tag{12}$$

where $\dot{q} = s + (\dot{q}_d - \Lambda e)$.

Substituting (5)-(6) into (12), we have

$$\begin{aligned}\dot{V}(t) &= s^T[(\hat{D} - D)(\ddot{q}_d - \Lambda\dot{e}) + (\hat{C} - C)(\dot{q}_d - \Lambda e) \\ &\quad + (\hat{G} - G) + u_r + u_f - Cs - \tau_d] \\ &\quad + \frac{1}{2}s^T\dot{D}s + \tilde{P}^T\Gamma\dot{\tilde{P}} \\ &= s^T(\tilde{D}\ddot{q}_r + \tilde{C}\dot{q}_r + \tilde{G} + u_r + u_f - Cs - \tau_d) \\ &\quad + \frac{1}{2}s^T\dot{D}s + \tilde{P}^T\Gamma\dot{\tilde{P}}\end{aligned} \tag{13}$$

where $\tilde{D} = \hat{D} - D$, $\tilde{C} = \hat{C} - C$, $\tilde{G} = \hat{G} - G$.

According to the kinetic characteristics of the robotic system (1) [28], we have

$$\tilde{D}(q)\ddot{q}_r + \tilde{C}(q, \dot{q})\dot{q}_r + \tilde{G}(q) = \Phi^T(q, \dot{q}, \dot{q}_r, \ddot{q}_r)\,\tilde{P} \tag{14}$$

Substituting (14) into (13), we have

$$\begin{aligned}\dot{V}(t) &= s^T(\Phi\tilde{P} + u_r + u_f - Cs - \tau_d) + \frac{1}{2}s^T\dot{D}s + \tilde{P}^T\Gamma\dot{\tilde{P}} \\ &= s^T(\Phi\tilde{P} + u_f) + s^T(u_r - \tau_d) + \frac{1}{2}s^T(\dot{D} - 2C)s \\ &\quad + \tilde{P}^T\Gamma\dot{\tilde{P}}\end{aligned} \tag{15}$$

According to the Property 2, we have

$$s^T(\dot{D} - 2C)s = 0 \tag{16}$$

Substituting (8)-(9) and (16) into (15), we have

$$\begin{aligned}\dot{V}(t) &= s^T(\Phi\tilde{P} + u_f) + s^T(u_r - \tau_d) + \tilde{P}^T\Gamma\dot{\tilde{P}} \\ &= \tilde{P}^T\Phi^T s + s^T u_f + s^T(u_r - \tau_d) + \tilde{P}^T\Gamma\dot{\tilde{P}} \\ &= s^T u_f + s^T(u_r - \tau_d) \\ &= -s^T K_f s + s^T(u_r - \tau_d) \\ &\leq s^T(u_r - \tau_d)\end{aligned} \tag{17}$$

Substituting (7) into (17), we have

$$\begin{aligned}\dot{V}(t) &\leq s^T\left[-\kappa_1|s|^{\frac{1}{2}}sgn(s) - \int \kappa_2 sgn(s)\, dt - \tau_d\right] \\ &= -s^T\kappa_1\sqrt{|s|}sgn(s) - s^T\int \kappa_2 sgn(s)\, dt - s^T\tau_d \\ &\leq -\kappa_1\left|s^T\right|\sqrt{|s|} - \left|s^T\right|\int \kappa_2 dt + \left|s^T\right|\left|\int \dot{\tau}_d dt\right| \\ &\leq -\kappa_1\left|s^T\right|\sqrt{|s|} - \left|s^T\right|\int \kappa_2 dt + \left|s^T\right|\int |\dot{\tau}_d|\, dt\end{aligned} \tag{18}$$

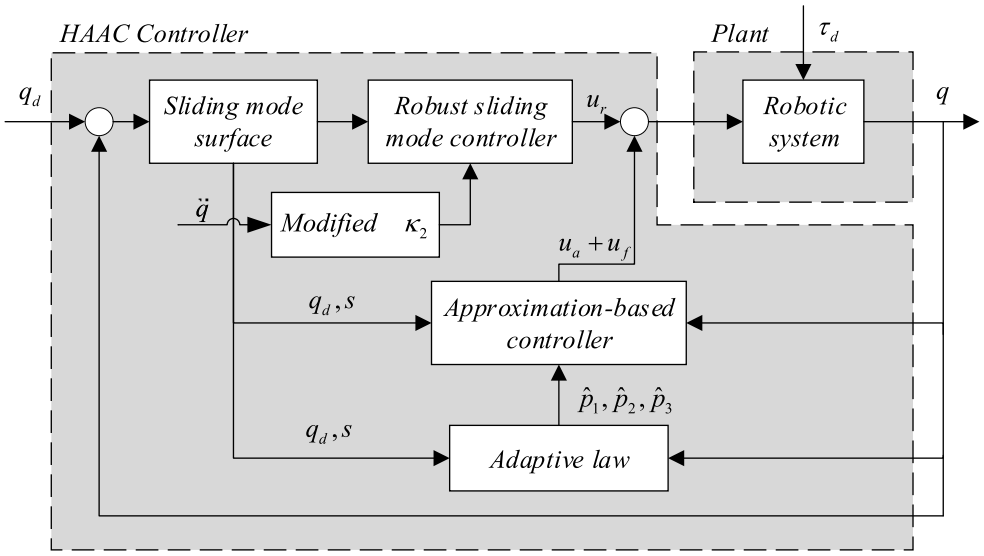

FIGURE 1. Control structure of the hybrid adaptive approximation-based control (HAAC) method.

If κ_2 satisfies the constraint conditions such that $|\dot{\tau}_d| \leq \varepsilon_d < \kappa_2$, we have

$$\begin{aligned}\dot{V}(t) &\leq -\kappa_1 \left|s^T\right| \sqrt{|s|} - \left|s^T\right| \int \kappa_2 dt + \left|s^T\right| \int \varepsilon_d dt \\ &= -\kappa_1 \left|s^T\right| \sqrt{|s|} - \left|s^T\right| \int (\kappa_2 - \varepsilon_d)\, dt \\ &\leq -\kappa_1 \left|s^T\right| \sqrt{|s|} \\ &\leq 0 \end{aligned} \tag{19}$$

According to (19), the following theorem is established to show the stability result of the robotic joints system given by (1). The control structure of the proposed HAAC method is shown in Fig. 1.

Theorem: For the robotic joints system described by (1), under the Properties 1-4, driven by the hybrid adaptive approximation-based controller (5)-(9), we can conclude that the global asymptotic stability of the closed-loop system is achieved if one has $\kappa_2 > \varepsilon_d > |\dot{\tau}_d|$.

III. SIMULATION RESULTS

In this section, the effectiveness of the proposed controller (5)-(9) is verified for a two-joint robotic system with two rotary degree of freedom. The robotic system is defined by a second-order nonlinear differential equation as described in (1), where $q = \left[q_1\ q_2\right]^T$, $\dot{q} = \left[\dot{q}_1\ \dot{q}_2\right]^T$ and $\ddot{q} = \left[\ddot{q}_1\ \ddot{q}_2\right]^T$.

The inertia matrix $D(q)$, centrifugal and Coriolis torques $C(q, \dot{q})$ and gravitational torques $G(q)$ are given as follows [3], [30]:

$$D(q) = \begin{bmatrix} p_1 + p_2 + 2p_3 \cos q_2 & p_2 + p_3 \cos q_2 \\ p_2 + p_3 \cos q_2 & p_2 \end{bmatrix} \tag{20}$$

$$C(q, \dot{q}) = \begin{bmatrix} -p_3 \dot{q}_2 \sin q_2 & -p_3(\dot{q}_1 + \dot{q}_2) sin q_2 \\ p_3 \dot{q}_1 \sin q_2 & 0 \end{bmatrix} \tag{21}$$

$$G(q) = \begin{bmatrix} p_1 g_1 \cos q_2 + p_3 g_1 \cos(q_1 + q_2) \\ p_3 g_1 \cos(q_1 + q_2) \end{bmatrix} \tag{22}$$

where $P = \left[p_1\ p_2\ p_3\right]^T$ is the model parameters, $g_1 = g/l_1$, g is the gravity acceleration, $g = 9.8m/s^2$. l_i and m_i are the length and mass of link i, where $l_1 = 1.3m$, $l_2 = 1m$, $m_1 = 2.910kg$, $m_2 = 3.957kg$, $i = 1, 2$.

The desired trajectory is selected as follows:

$$q_d = \begin{bmatrix} q_{d1} \\ q_{d2} \end{bmatrix} = \begin{bmatrix} \sin(2\pi t) \\ \cos(2\pi t) \end{bmatrix} \tag{23}$$

The initial conditions are given as follows:

$$q(0) = \left[1.0 \quad 0.1\right]^T, \quad \dot{q}(0) = \left[0 \quad 0\right]^T \tag{24}$$

The external disturbance is given as follows:

$$\tau_d = \begin{bmatrix} \tau_{d1} \\ \tau_{d2} \end{bmatrix} = \begin{bmatrix} 3\dot{q}_1 \sin t \\ 3\dot{q}_2 \cos t \end{bmatrix} \tag{25}$$

The actual model parameters of robotic system are given as $p_1 = 11.6052\ kg \cdot m^2$, $p_2 = 3.9570\ kg \cdot m^2$, and $p_3 = 5.1441\ kg \cdot m^2$. The sliding mode coefficient Λ and positive definite matrix Γ are chosen as $\Lambda = diag(5, 5)$, and $\Gamma = diag(5, 5, 5)$.

For comparison, we have introduced other methods in the following case 1 and case 2. The simulations of the proposed control is given in the case 3. The objective of simulations is to examine whether the proposed control method is able to reduce the tracking errors and the chattering compared with the comparative methods. The simulation results are given in Figs. 2-9.

A. CASE 1: PD APPROXIMATION-BASED CONTROL (PD-AC)

Considering the PD control in [6] and [31], the PD approximation-based controller is given as:

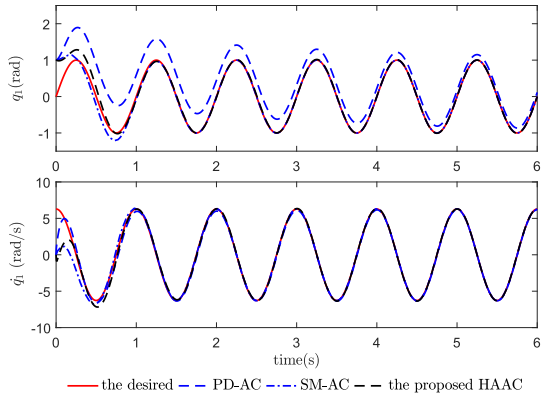

FIGURE 2. The position and velocity tracking of link 1.

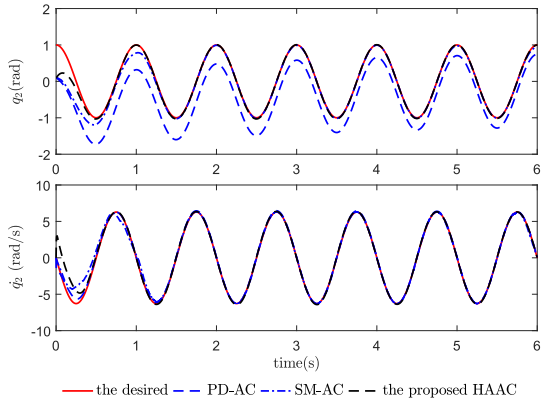

FIGURE 3. The position and velocity tracking of link 2.

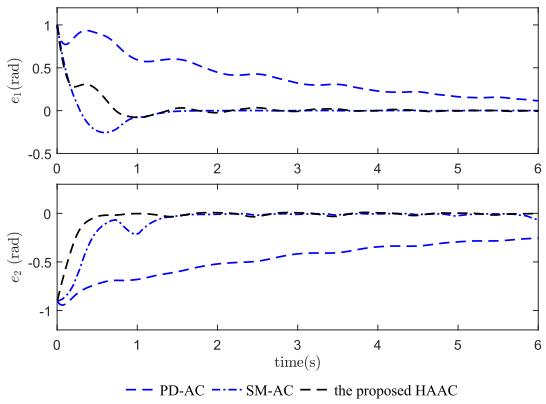

FIGURE 4. The position tracking errors of link 1 and link 2.

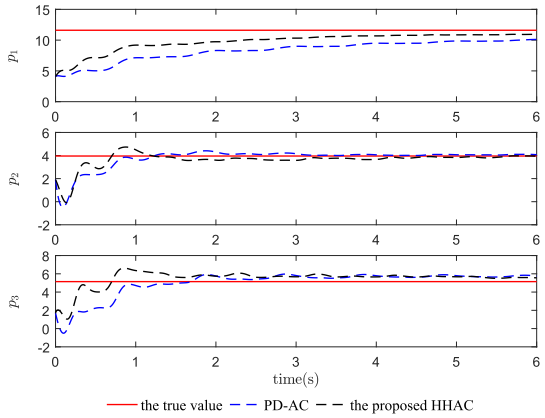

FIGURE 5. The approximate results of the model parameters.

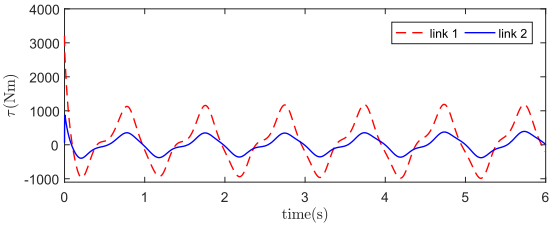

FIGURE 6. Control torques with the PD-AC.

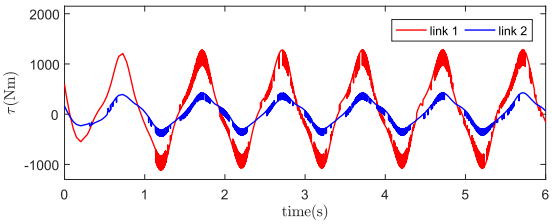

FIGURE 7. Control torques with the SM-AC.

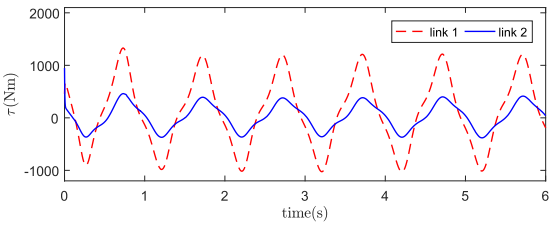

FIGURE 8. Control torques with the proposed HAAC.

$\tau = -K_p e - K_d \dot{e} + \hat{D}\ddot{q}_d + \hat{C}\dot{q}_d + \hat{G}$, where $\dot{\hat{P}} = -\Gamma^{-1}\Phi^T(q, \dot{q}, \dot{q}_d, \ddot{q}_d)\dot{e}$, $K_p = diag\,(150, 150)$, and $K_d = diag\,(550, 550)$.

Figs. 2-4 show the position tracking, velocity tracking and position errors of link 1 and link 2, respectively. Fig. 5 shows the approximate results of the model parameters of robotic system, and Fig. 6 gives the control input torques. From Figs. 2-4, it is obvious that the PD-AC has a large position tracking error from link 1 or link 2. Moreover, link 1 has a very lager initial torque in Fig. 6.

B. CASE 2: SLIDING MODE APPROXIMATION-BASED CONTROL (SM-AC)

Considering the SMC in [8] and [32], the sliding mode approximation-based controller is given as: $\tau = K_s sgn\,(s) + s + \hat{D}\ddot{q}_r + \hat{C}\dot{q}_r + \hat{G}$, where $\dot{\hat{P}} = 0.95P$, $K_s = diag\,(k_{s11}, k_{s22})$, $k_{sii} = \sum_{j=1}^{3} \bar{\phi}_{ij} \cdot \zeta_j$, $\bar{\phi}_{ij} = |\phi_{ij}| + 0.1$, $\zeta_j = |\tilde{p}_j| + 0.5$, $\phi_{ij} \in \Phi\,(q, \dot{q}, \dot{q}_r, \ddot{q}_r)$, and $j = 1, 2, 3$.

Figs. 2-4 show the position tracking, velocity tracking and position errors of link 1 and link 2, respectively. Fig. 7 shows

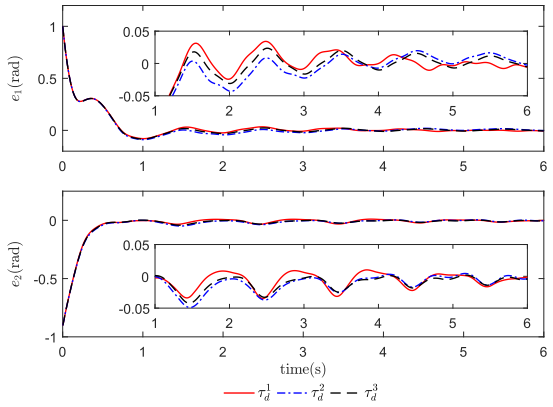

FIGURE 9. The position errors of link 1 and link 2 with different disturbances.

the control input torques. Obviously, the SM-AC has severe chattering due to the introduction of the discontinuities term $sgn(s)$. Compared to the case 1, the position tracking effect is much better. In this case, there is no adaptive term for adjusting the robotic parameters in real time.

C. CASE 3: THE PROPOSED HAAC

In this case, the proposed HAAC controller is tested. The control gain K_f is given such that $K_f = diag(200, 200)$. κ_2 is given by the (29), and $\kappa_1 = 5$, $\delta = 0.1$.

Figs. 2-4 show the position tracking, velocity tracking and position errors of link 1 and link 2, respectively. Fig. 5 shows the approximate results of the model parameters, and Fig. 8 gives the control input torques. In this case, we use the super-twisting algorithm to design the robust controller, which successfully decrease the chattering in the input torques compared to the case 2, and the fluctuation of input torques is more stable than the case 1.

From Figs. 2-4, it is obvious that the proposed HAAC has a faster response time in term of the position tracking compared to the case 1 and case 2, i.e., the position errors will converge to zero in a shorter time. The velocity is the derivative of position, thus these three control methods have similar velocity tracking effects. From Fig. 5, the proposed HAAC has a better approximation effect on p_1 compared to the case 1.

D. CASE 4: DISTURBANCES TEST

To verify the robustness of the proposed controller to external disturbances, three different forms of disturbances are tested in this case. These three disturbances are given as follows:

$$\tau_d^1 = \begin{bmatrix} 3\dot{q}_1 \sin t \\ 3\dot{q}_2 \cos t \end{bmatrix} \tag{26}$$

$$\tau_d^2 = \begin{bmatrix} 10 \sin t \\ 10 \sin t \end{bmatrix} \tag{27}$$

$$\tau_d^3 = \begin{bmatrix} \dot{q}_1 + 2 \sin (q_1) \\ 0.7\dot{q}_2 + 0.5 \sin (q_2) \end{bmatrix} \tag{28}$$

where τ_d^1 is given in this paper, τ_d^2 is given in [3] and τ_d^3 is given in [10], respectively.

Fig. 9 gives the position errors of link 1 and link 2. Furthermore, we can conclude that the proposed controller is robust to these three different forms of external disturbances. By selecting the control parameters appropriately, the position errors will eventually converge to a small neighborhood around zero.

Remark: According to (19), the control parameter κ_2 designed in the robust controller (7), is chosen such that $\kappa_2 > |\tilde{\tau}_d|$. However, in order to ensure the stability of the closed-loop system, κ_2 is usually chosen to be conservatively large. This is not desirable due to the chattering introduced. Considering the external disturbances described in (26), κ_2 can be changed to

$$\kappa_{2i} = 3 \left(\max \{|\ddot{q}_i|\} + \max \{|\dot{q}_i|\}\right) + \delta \tag{29}$$

where $\delta \in \mathbb{R}^+$ is a small constant, $i = 1, 2$. The modified parameter κ_{2i} only subject to the output of each link, rather than choosing a relatively large constant. This improvement diminishes the value of the control parameter κ_2 and does not affect the stability. It is also a viable way to decrease the chattering.

IV. ROBOTIC JOINTS TEST

The torsional vibration performance can be expressed as the effective value of the torsional vibration acceleration (or displacement) of RV reducer at different speeds [33]. In this experiment, the acceleration signal of the torsional vibration is measured by using a sensor. The velocity and displacement signal are obtained by integrating of acceleration.

A. TEST DEVICES

As shown in Fig. 10, the test devices consist of the vibration sensor, rotating arm, RV reducer, servo motor, and support frame.

The vibration sensor adopts the three-directional piezoelectric acceleration sensors, which the model number is MTE-T8 and the sampling frequency is 800Hz. The sensor is used to collect the vibration signals of the axial, radial and circumferential direction of the measuring point. In engineering, the circumferential signal is usually regarded as the torsional vibration. A counterweight is added to simulate the operation of industrial robotic joints under the rotational inertia. The relevant parameters of the rotating arm are shown in Table 1.

TABLE 1. The parameters of the rotating arm.

Mass	Length	Counter weight	Rotational inertia
$58.2kg$	$1.3m$	$79.14kg$	$56.65kg \cdot m^2$

B. ACCELERATION SIGNAL PROCESSING

In order to obtain the accurate velocity and displacement signal of the torsional vibration, the method shown in Fig. 10 is designed to deal with the original acceleration signal.

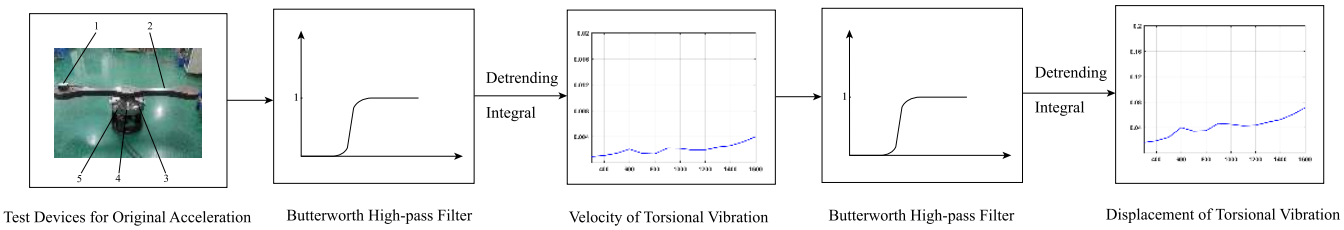

FIGURE 10. The test devices and signal processing. In the test devices: 1-vibration sensor, 2-rotating arm, 3-RV reducer, 4-servo motor, and 5-support frame.

The low frequency part of the vibration signal affects the amplitude of the displacement of torsional vibration. The zero drift caused by the temperature change contains the trend term, which affects the accuracy of speed and displacement in the integration transformation [34], [35]. Thus, it is essential to eliminate the trend item in the original acceleration signal. Moreover, the Butterworth high-pass filter is introduced to eliminate the direct current (DC) component and noise disturbances.

C. TEST RESULTS

The model of RV reducer in the experiment is 20E-15420. The SM-AC is not considered because there has severe chattering in its control torque compared to the PD-AC and the proposed HAAC. Due to the inverse ration between the output torques of the motor and the rotational speed, the minimum speed of the motor is designed to be 300 rpm when the control input of the PD-AC is maximum. From Figs. 6 and 8, it can be seen that the maximum control torque of PD-AC is about twice that of the proposed HAAC. Thus, the minimum speed of the motor of the proposed HAAC is designed to be 600 rpm. The maximum speed of the motor of these two controllers are all designed to be 1600 rpm. Experiment results are shown in the Fig. 11 and Table 2.

TABLE 2. The mean and variance.

Controller	PD-AC	The proposed HAAC
The speed of motor	300rpm-1600rpm	600rpm-1600rpm
Average Acceleration	$0.0149g$	$0.0162g$
Average Displacement	0.0413mm	0.0471mm
Variance of Acceleration	2.0019×10^{-5}	1.7118×10^{-5}
Variance of Displacement	2.2591×10^{-4}	1.1835×10^{-4}

Fig. 11 shows the variation of the acceleration and displacement of the torsional vibration. Table 2 gives the mean and variance of the acceleration and displacement. It can be seen that the average acceleration and average displacement of the PD-AC is smaller than the proposed HAAC. However, the variance of acceleration and displacement is larger than the proposed HAAC. The variance reflects the fluctuation of the torsional vibration signal, i.e., the fluctuation of the torsional vibration signal of the PD-AC is larger than the proposed HAAC. It means that the torsional vibration of the RV reducer under the action of the PD-AC is more severe than that of the proposed HAAC. It is not conducive to improving the accuracy of the trajectory tracking of robotic manipulator joints.

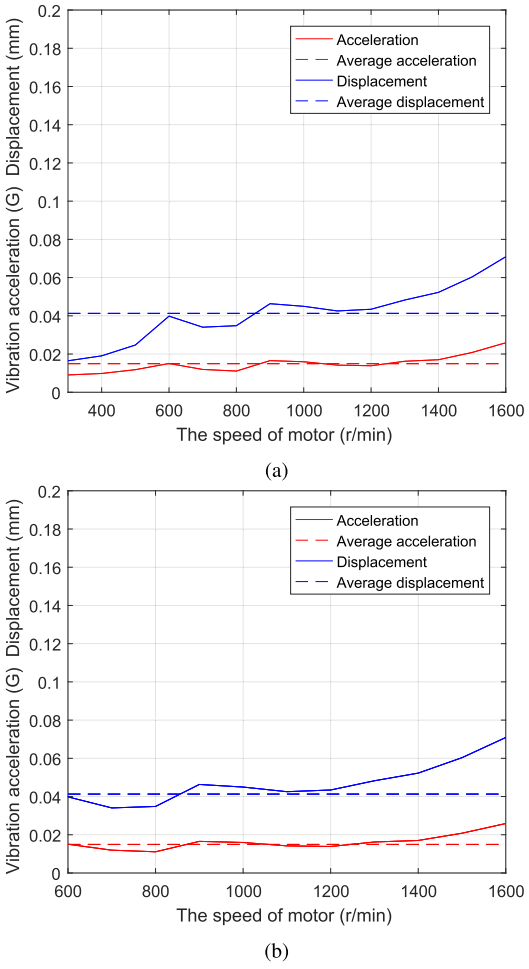

FIGURE 11. The vibration acceleration and displacement. (a) The PD-AC. (b) The proposed HAAC.

V. CONCLUSIONS AND FURTHER WORK

This paper presents a hybrid adaptive approximation-based control (HAAC) method to deal with the problem of trajectory tracking for a class of robotic joints system. The actual robotic model parameters are estimated by using an adaptive approximation-based controller. The chattering is successfully decreased by using the super-twisting algorithm

and modified robust control parameters. The stability of the closed-loop system has been proved by using Lyapunov theory. In the simulation experiment, the proposed controller is compared to the PD approximation-based controller and sliding mode approximation-based controller, respectively. A disturbance test has verified the robustness of the proposed controller. From the simulation results for a two-joint robotic system, we can obtain the following conclusions: 1) the proposed controller is able to track the desired trajectory with the smaller tracking errors than the comparison controllers; 2) the tracking errors eventually converge to a small neighborhood around zero; 3) the designed robust controller has successfully decreased the chattering; 4) the proposed controller is robust to the external disturbances. Moreover, this paper also presents a torsional vibration experiment on the RV reducer to test the influence of the control torques of the proposed controller. Test results has proved that the torsional vibration of the RV reducer with the proposed controller is much smaller. It is more conducive to achieving the better trajectory tracking performance and ensuring the stability of robotic system.

In conclusion, the proposed controller is more effective and practical for dealing with a class of robotic joints system with the uncertainties. Further works will focus on extending the results of this study to test multiple joints of robotic system.

APPENDIX

According to (20)-(22), the inertia matrix $D(q)$, centrifugal and Coriolis torques $C(q, \dot{q})$ and gravitational torques $G(q)$ are defined as

$$D(q) = \begin{bmatrix} p_1 + p_2 + 2p_3 \cos q_2 & p_2 + p_3 \cos q_2 \\ p_2 + p_3 \cos q_2 & p_2 \end{bmatrix}$$

$$C(q, \dot{q}) = \begin{bmatrix} -p_3 \dot{q}_2 \sin q_2 & -p_3(\dot{q}_1 + \dot{q}_2) sin q_2 \\ p_3 \dot{q}_1 \sin q_2 & 0 \end{bmatrix}$$

$$G(q) = \begin{bmatrix} p_1 g_1 \cos q_2 + p_3 g_1 \cos(q_1 + q_2) \\ p_3 g_1 \cos(q_1 + q_2) \end{bmatrix}$$

Let

$$P = \begin{bmatrix} p_1 & p_2 & p_3 \end{bmatrix}^T$$

where $p_1 = (m_1 + m_2) l_1^2$, $p_2 = m_2 l_2^2$ and $p_3 = m_2 l_1 l_2$ are the model parameters of robotic system.

In fact, due to the interaction between robot and environment, it is difficult to obtain the precise values of p_1, p_2 and p_3. Therefore, the estimated values of P is introduced in the approximation-based controller (6).

$$\hat{P} = \begin{bmatrix} \hat{p}_1 & \hat{p}_2 & \hat{p}_3 \end{bmatrix}^T$$

where $\hat{p}_1$, $\hat{p}_2$ and $\hat{p}_3$ are the estimated values of p_1, p_2 and p_3, respectively. $\hat{P}$ is given by using the adaptive controller (9).

Therefore, the estimated terms $\hat{D}$, $\hat{C}$ and $\hat{G}$ in the approximation-based controller (6) are given as follows:

$$\hat{D}(q) = \begin{bmatrix} \hat{p}_1 + \hat{p}_2 + 2\hat{p}_3 \cos q_2 & \hat{p}_2 + \hat{p}_3 \cos q_2 \\ \hat{p}_2 + \hat{p}_3 \cos q_2 & \hat{p}_2 \end{bmatrix}$$

$$\hat{C}(q, \dot{q}) = \begin{bmatrix} -\hat{p}_3 \dot{q}_2 \sin q_2 & -\hat{p}_3(\dot{q}_1 + \dot{q}_2) sin q_2 \\ \hat{p}_3 \dot{q}_1 \sin q_2 & 0 \end{bmatrix}$$

$$\hat{G}(q) = \begin{bmatrix} \hat{p}_1 g_1 \cos q_2 + \hat{p}_3 g_1 (q_1 + q_2) \\ \hat{p}_3 g_1 (q_1 + q_2) \end{bmatrix}$$

The proof is completed.

ACKNOWLEDGEMENT

The authors would like to thank the anonymous reviewers for their constructive comments that helped to improve the quality of this paper.

REFERENCES

[1] X. P. Shi and S. R. Liu, "A survey of trajectory tracking control for robot manipulators," *Control Eng. China*, vol. 18, no. 1, pp. 116–122, and 132, Jun. 2011.

[2] P. R. Ouyang, W. J. Zhang, and M. M. Gupta, "An adaptive switching learning control method for trajectory tracking of robot manipulators," *Mechatronics*, vol. 16, no. 1, pp. 51–61, Feb. 2006.

[3] Y. Pan, Y. Liu, B. Xu, and H. Yu, "Hybrid feedback feedforward: An efficient design of adaptive neural network control," *Neural Netw.*, vol. 76, pp. 122–134, Apr. 2016.

[4] Y. Pan and H. Yu, "Biomimetic hybrid feedback feedforward neural-network learning control," *IEEE Trans. Neural Netw. Learn. Syst.*, vol. 28, no. 6, pp. 1481–1487, Jun. 2017.

[5] J. J. Rubio *et al.*, "Learning of operator hand movements via least angle regression to be teached in a manipulator," *Evolving Syst.*, to be published. doi: 10.1007/s12530-018-9224-1.

[6] J. D. J. Rubio, E. Garcia, A. Aquino, C. Aguilar-Ibañez, J. Pacheco, and J. A. Meda-Campana, "Recursive least squares for a manipulator which learns by demonstration," *Rev. Iberoamer. Autom. Inform. Ind.*, Jul. 2018. doi: 10.4995/riai.2018.8899.

[7] J. S. Guan, C. M. Lin, G. L. Ji, L. W. Qian, and Y. M. Zheng, "Robust adaptive tracking control for manipulators based on a TSK fuzzy cerebellar model articulation controller," *IEEE Access*, vol. 6, pp. 1670–1679, Feb. 2018.

[8] J. D. J. Rubio, "Robust feedback linearization for nonlinear processes control," *ISA Trans.*, vol. 74, pp. 155–164, Mar. 2018.

[9] J. K. Liu and F.-C. Sun, "Research and development on theory and algorithms of sliding mode control," *Control Theory Appl.*, vol. 24, no. 3, pp. 407–418, Jun. 2007.

[10] M. D. Tran and H. J. Kang, "A novel adaptive finite-time tracking control for robotic manipulators using nonsingular terminal sliding mode and RBF neural networks," *Int. J. Precis. Eng. Manuf.*, vol. 17, no. 7, pp. 863–870, Jul. 2016.

[11] S. Islam and X. P. Liu, "Robust sliding mode control for robot manipulators," *IEEE Trans. Ind. Electron.*, vol. 58, no. 6, pp. 2444–2453, Jun. 2011.

[12] H. Wang, Y. Pan, S. Li, and H. Yu, "Robust sliding mode control for robots driven by compliant actuators," *IEEE Trans. Control Syst. Technol.*, to be published.

[13] Y. Pan, X. Li, H. Wang, and H. Yu, "Continuous sliding mode control of compliant robot arms: A singularly perturbed approach," *Mechatronics*, vol. 52, pp. 127–134, Jun. 2018.

[14] W. He, Y. Chen, and Z. Yin, "Adaptive neural network control of an uncertain robot with full-state constraints," *IEEE Trans. Cybern.*, vol. 46, no. 3, pp. 620–629, 2016.

[15] C. K. Lin, "Nonsingular terminal sliding mode control of robot manipulators using fuzzy wavelet networks," *IEEE Trans. Fuzzy Syst.*, vol. 14, no. 6, pp. 849–859, Nov. 2006.

[16] A. Tayebi, S. Abdul, M. B. Zaremba, and Y. Ye, "Robust iterative learning control design: Application to a robot manipulator," *IEEE/ASME Trans. Mechatronics*, vol. 13, no. 5, pp. 608–613, Oct. 2008.

[17] Z. H. Min and H. L. Chen, "Research on RBFNN adaptive sliding mode control of serial manipulators," *J. Heilongjiang Univ. Sci. Technol.*, vol. 27, no. 2, pp. 149–153, Mar. 2017.

[18] A. G. Wang and Q. D. Wang, "Design of fuzzy-adaptive sliding mode control system for flexible series manipulator," *J. Hefei Univ. Technol.*, vol. 40, no. 5, pp. 601–605 and 659, May. 2017.

[19] L. G. Jiang and J. Z. Zhang, "An adaptive control approach for manipulator," *Ship Sci. Technol.*, vol. 36, no. 6, pp. 129–133, Jun. 2014.

[20] C. Zhang and Z. Zhang, "Application of adaptive fuzzy robust control in manipulator system," *Autom. Appl.*, no. 5, pp. 126–128, May 2017.

[21] L. P. Xi, Z. L. Chen, and X. M. Li, "Design of a sliding mode control scheme based on improved exponent trending law for robotic manipulators," *Electron. Opt. Control*, vol. 19, no. 4, pp. 47–49 and 54, Apr. 2012.
[22] B. Mezghani, N. Romdhane, and T. Damak, "Adaptive terminal sliding mode control for rigid robotic manipulators," *Int. J. Autom. Comput.*, vol. 8, no. 2, pp. 215–220, 2011.
[23] S. Liu, Y. Wang, H. Fang, and Q. Xu, "Trajectory tracking sliding mode control for robot," *Microcomput. Inf.*, no. 17, pp. 261–262, Jun. 2008.
[24] S. Wang, L. Yu, J. Xu, K. Xing, and Z. Wang, "Adaptive robust tracking control for robotic manipulators," *Control Eng. China*, vol. 22, no. 2, pp. 241–245, Mar. 2015.
[25] R. Han and X. Liu, "Adaptive fuzzy sliding mode control of phantom Omni robot," *Appl. Res. Comput.*, vol. 35, no. 11, pp. 3335–3337 and 3342, Nov. 2018.
[26] A. T. M. Amin, A. H. A. Rahim, and C. Y. Low, "Adaptive controller algorithm for 2-DOF humanoid robot arm," *Procedia Technol.*, vol. 15, pp. 765–774, Jan. 2014.
[27] W. He, S. S. Ge, Y. Li, E. Chew, and Y. S. Ng, "Neural network control of a rehabilitation robot by state and output feedback," *J. Intell. Robot. Syst.*, vol. 80, no. 1, pp. 15–31, 2015.
[28] X. H. Jiao, Y. F. Li, Y. M. Fang, and Q. S. Geng, "A robust adaptive control method for robot," *Robot Techn. Appl.*, no. 3, pp. 40–43, May. 2002.
[29] H. Liu and T. Zhang, "Adaptive neural network finite-time control for uncertain robotic manipulators," *J. Intell. Robot. Syst.*, vol. 75, nos. 3–4, pp. 363–377, 2014.
[30] C. Y. Su and T. P. Leung, "A sliding mode controller with bound estimation for robot manipulators," *IEEE Trans. Robot. Autom.*, vol. 9, no. 2, pp. 208–214, Apr. 1993.
[31] J. K. Liu, "Adaptive robust control for robot," in *Disgenic of Robot Control System and MATLAB Simulation*. Beijing, China: Tsinghua Univ. Press, 2008, pp. 531–537.
[32] J. Liu, "Sliding mode control for robot," in *Disgenic of Robot Control System and MATLAB Simulation*. Beijing, China: Tsinghua Univ. Press, 2008, pp. 445–448.
[33] D. S. Huang, J. L. Liu, and J. J. Gu, "Research of the test and diagnosis of torsional vibration of RV reducer," *J. Mech. Transmiss.*, vol. 40, no. 10, pp. 70–73, Oct. 2016.
[34] D. W. Li, X. Y. Xiong, and B. Li, "Research on the processing of vibration acceleration signal," *Mech. Elect. Eng. Technol.*, vol. 37, no. 9, pp. 50–52 and 126, Sep. 2008.
[35] M. K. Gu and Z. H. Lu, "Identification of a mechanism's vibration velocity and displacement based on the acceleration measurement," *Mech. Sci. Technol. Aerosp. Eng.*, vol. 30, no. 4, pp. 522–526, Apr. 2011.

BIN REN received the B.S. and M.S. degrees in mechanical science and engineering from Northeast Petroleum University, in 2004 and 2007, respectively, and the Ph.D. degree in mechanical engineering from Zhejiang University, Zhejiang, China, in 2010.

From 2011 to 2013, she was a Postdoctoral Research Fellow with the Computer Application Program, Zhejiang University. In 2012, she was as a Visiting Scholar with the Mechanical Engineering Department, California State University, Sacramento. From 2014 to 2016, she was as a Postdoctoral Researcher with the Department of Architectural and Civil Engineering, City University of Hong Kong, Hong Kong. She is currently a member of the Shanghai Key Laboratory of Intelligent Manufacturing and Robotics. She served as a Principal Investigator of two projects from the National Natural Science Foundation of China and of three projects from the Ministry of Sciences and Technology of China. She has published more than 20 articles and developed two copyrights of computer software. Her research interests include product digital design, virtual prototype simulation, and hybrid control computer.

Dr. Ren's awards and honors include the Young Eastern Scholar of Shanghai and the Hong Kong Scholar. She is a member of the Society of Hong Kong Scholars.

YAO WANG received the B.S. degree in mechanical design, manufacturing, and automation from Shanghai Ocean University, Shanghai, China, in 2017. He is currently pursuing the M.S. degree in mechanical engineering from Shanghai University, Shanghai.

His research interests include robotics, adaptive control, and sliding mode control systems.

XURONG LUO received the B.S. degree in mechanical design, manufacturing, and automation from Nanchang Hangkong University, Nanchang, China, in 2016. He is currently pursuing the M.S. degree in mechanical engineering from Shanghai University, Shanghai, China.

His research interests include exoskeleton robot, dynamics modeling, and simulation.

ROGELIO LOZANO received the B.S. degree in electronic engineering from the National Polytechnic Institute of Mexico, in 1975, the M.S. degree in electrical engineering from the Centro de Investigación y de Estudios Avanzados (CINVESTAV), Mexico, in 1977, and the Ph.D. degree in automatic control from the Laboratoire d'Automatique de Grenoble, France, in 1981.

From 1985 to 1987, he was the Head of the Section of Automatic Control. He was the Head of the Heudiasyc Laboratory, from 1995 to 2007. Since 1990, he has been the Research Director with the Centre National de la Recherche Scientifique (CNRS), University de Technology of Compiègne, France. He is currently the Head of the Joint Mexican–French UMI 3175 CNRS. He has been an advisor or co-advisor of more than 35 Ph.D. theses. He has coordinated or participated in numerous French projects dealing with UAVs. He has published more than 130 international journal papers and ten books. His research interests include UAVs, mini-submarines, exo-squelettons, and automatic control.

Dr. Lozano has recently organized two international workshops on UAVs (IFAC RED UAS 2013 and the IEEE RAS RED UAS 2015). He has been participating in the organization of the annual international conference, International Conference on Unmanned Aerial Systems (ICUAS), since 2010. He was an Associate Editor of *Automatica*, from 1987 to 2000. He is an Associate Editor of the *International Journal of Adaptive Control and Signal Processing* and the *Journal of Intelligent and Robotics Systems*.